Chapter 6

Lateral Shearing Digital Holography Microscopy of Immobilized Cells

In previous chapters, we have discussed quantitative phase contrast microscopy in which sample was prepared by making blood smear on a standard 1mm glass slide. It is quite certain that RBC's morphology will change as its osmolarity is not maintained. To study the cells in their own natural environment that is in fluids one has to immobilize the cells. In 1970, Arthur Ashkin, a scientist working at Bell Laboratories discovered a very peculiar effect of radiation on micrometer sized particle. He was able to demonstrate that small particles (of micrometer diameter) can be manipulated and their movement can be constrained using radiation pressure [110]. In 1986, he demonstrated that by focusing laser beam to a narrow spot (tight focusing), the micron sized particle such as polystyrene beads are attracted towards the center of the focused laser spot [111]. The tightly focused laser beam provides enough force (order of piconewtons), which is capable of trapping micron sized particle in three dimensions (lateral and axial). This setup was later known by the name Optical Tweezer (since it is able to hold the particle in a particular position just like a mechanical tweezer). Light can impart force to matter by absorption, scattering and emission of radiation. Among these, the most familiar form is the scattering force, defined as the force due to scattering of light by matter. The scattering process can be classified into different models such as Mie regime (particle size is larger than laser light wavelength) [112] and Raleigh regime (particle size is smaller than laser wavelength) [113] depending on the test object size with respect to laser wavelength. The principle of optical tweezer is based on interaction (momentum exchange) between tightly focused laser beam and micron sized test object by means of light scattering. This scattering force is proportional to the intensity of the light and acts along the direction of the propagation of the light. Due to conservation of momentum, the transparent object experiences a gradient force when it comes in the vicinity of the focused light spot. This means that the direction of scattering force (axial) is towards the direction of propagation of the beam and the gradient force (lateral) is towards the focal point of the focusing lens, which produces the focused laser beam. The strength of the optical tweezer is proportional to the power of the laser source and also physical and optical parameters (size, shape and refractive index) of the trapped particle.

In the recent years, in physics and biological applications, optical tweezers have become powerful tool for micro-manipulation of cells and technical objects. Optical tweezers are capable of manipulating objects of size ranging from single atom to 100s of micrometer in diameter. For biomedical researchers and clinicians, optical tweezers have found to be important tool for studying stem cells [114-115], circulating tumor cells [116], infected cells [117], viruses and bacteria [118], cells for genetic testing [119], mechanics of single DNA molecule [120] and development of cell biosensors [121]. Optical tweezers are widely used for measuring elasticity, optical sorting of particles [122-125], measuring corner frequency of microscopic particles [126]. But unfortunately, Optical tweezers setup demands expensive optical, measurement and imaging components (e.g., high power laser, imaging system, Quadrant photo detector (QPD) etc.). The cost of commercially available optical tweezer setup is approximately USD 20000, which makes it an expensive tool for studying immobilized cells in fluids.

A low cost optical tweezer can be constructed using DVD optical pick-up units [127], which comprises of a red laser (λ=650nm) providing output powers up to 250mW and a short focal length focusing lens (used to burn DVDs) with high numerical aperture. This combination of laser and focusing lens makes it a potential option to construct low cost optical tweezers [127]. In this work described in this, a compact 3D-printed optical trapping device was developed using DVD Optical-pickup and was integrated with self-referencing lateral shearing DHIM. An indigenously developed QPD was also added to the device for measurement of cell fluctuations and trap stiffness while the cell in immobilized state. The device was tested on polystyrene micro-spheres and RBCs. In the case of RBCs, the sample was prepared in phosphate buffer saline solution (PBS) and by adding the bovine albumin serum to prevent agglomeration and adhesion of RBCs to the chamber walls.

6.1 Optical Tweezers

The operation of the Optical tweezer can be understood by studying the interaction of light with the dielectric particle and the forces acting on it. The laser beam which is used to trap the particle is focused by sending it through a high numerical aperture lens like a microscope objective. The beam waist (at the focal plane of the focusing lens) contains very strong electric field gradient. The light carries momentum in the direction of propagation and is proportional to its energy. The reflection and refraction of light at the interface changes the momentum of the light (momentum

transfer occurs). Dielectric objects are attracted along the gradient to the region of the strongest electric field, which is the center of the beam.

The radiation pressure is generally considered to comprise two components: scattering force and gradient force. The tightly focused laser beam has Gaussian profile and contains very strong electric field gradient (especially at the beam waist). When focused laser beam passes through an object, it reflects (scattered by the particle) resulting in a force in the direction of the incident beam (Fig. 6.1).

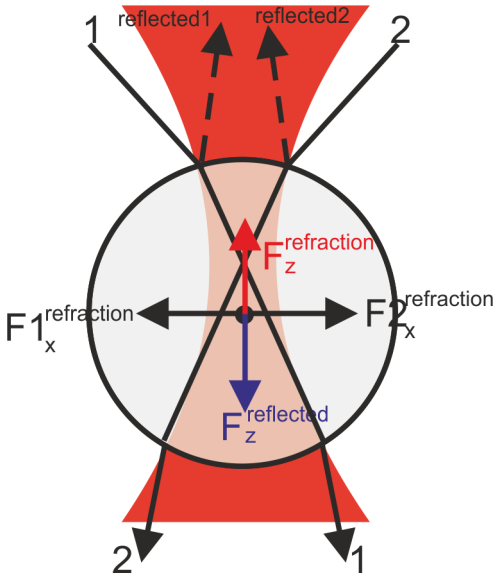

Fig. 6.1: Scattered (reflected) and refracted light work together to hold the particle at the same position.

This scattering force is results in the particle being slightly displaced form the exact position of the beam waist. The beam also refracts (bends) and changes its direction, again resulting in a change of momentum. For conservation of the total momentum, according to Newton's third law, the object undergoes an equal and opposite momentum change which leads to object experiencing a reaction force towards the focus of the beam (Fig. 6.1), this force is known as gradient force. The gradient force acts as an attractive force pushing the bead towards the region of greater light intensity. A ray tracing argument tell that (Fig. 2.1) the scattered light creates a scattering force in the direction of light propagation, while the refracted light creates an opposing gradient force. It can also be seen from Fig. 6.1 that due to the Gaussian profile of laser beam, the light ray at the center of the beam carries more photons than the light ray at the edges (outline) of the beam, resulting in a larger restoring force that pulls the particle into the center of the focal plane

(laterally). To form a stable object trap, the magnitude of gradient force should be greater than magnitude of scattering force.

Two different theoretical approaches are derived depending on the ratio of incident light wavelength (λ) and diameter (d) of the irradiated particle. When the diameter (*d*) of the trapped particle is greater than wavelength (λ) of the light (λ<<d), Mie/Ray optics approach is applied to the radiation pressure forces from scattering of incident light and the phenomenon can be explained using ray-optics picture. When the diameter of the particle is very less than wavelength of incident light (λ>>d), Rayleigh regime is applied and the particle acts as a dipole and the forces arise from dipole-field interactions. In the third intermediate regime, when the diameter of the particle is equal to wavelength of light, both of the above approaches fails to describe origin of forces in the optical trapping. In the present work, the particle dimension falls in the Mie/Ray regime so geometrical optics will be used to calculate Scattering force and Gradient force acting on the trapped particle [135].

6.2 Forces experienced by dielectric particle (Mie/Rayleigh regime)

Consider a dielectric particle having refractive index n_2 which is suspended in medium having refractive index n_1 ($n_2>n_1$). When light rays carrying momentum passes through the dielectric particle, it refracts and changes its direction at each and every point on the object. According to law of conservation of momentum, the rate of change of momentum in the bent rays transports an equal and opposite rate of change in momentum to the particle. Hence if the dielectric particle is perfect absorber, the force generated on the particle by incident light of power (P), due to transfer of momentum is given by [135]

$$F = \frac{n_1 P}{c} \tag{6.1}$$

If the dielectric particle is perfect reflector, the force generated on the particle by incident light of power (P)

$$F = \frac{2n_1 P}{c} \tag{6.2}$$

But, for optical tweezers, the trapped dielectric particle is neither perfect reflector nor perfect absorber, so the scattering force and gradient force can be given by [135]

$$F_{gradient} = \frac{n_1 P}{c}\left(R\sin 2\theta_i - \frac{T^2[\sin(2\theta_i - 2\theta_r) + R\sin 2\theta_i]}{1 + R^2 + 2R\cos 2\theta_r}\right) \tag{6.3}$$

$$F_{scattering} = \frac{n_1 P}{c}\left(1 + R\cos 2\theta_i - \frac{T^2[\cos(2\theta_i - 2\theta_i) + R\cos 2\theta_i]}{1 + R^2 + 2R\cos 2\theta_r}\right) \tag{6.4}$$

Where, θ_i and θ_r are the angles of incidence and refraction respectively, R and T are the reflectivity and transmissivity of the surface of the dielectric sphere and P is the incident power of the laser.

Using the conservation of the momentum, the stable optical trap is achieved by balancing of these two forces. In this case the force on the dielectric particle is defined as

$$F = \frac{Qn_1 P}{c} \tag{6.5}$$

where, Q is a dimensionless quantity which depends on size of trapped particle and refractive index difference between the particle and the medium.

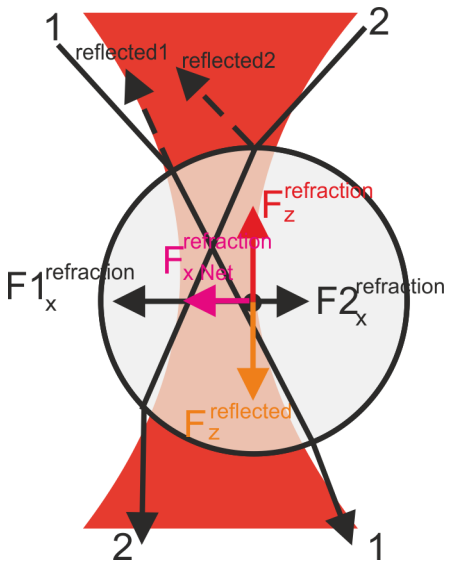

Fig. 6.2: A shift of the particle from the trapped position results in a net fore towards the region of higher intensity there by keeping the particle in the trapped position.

By using simple geometrical optics, shown in Fig. 6.2, the dielectric particle will experience two different forces $F_{1x}^{\text{refraction}}$ and $F_{2x}^{\text{refraction}}$ due to Gaussian intensity profile of the trapping beam. $F_{1x}^{\text{refraction}}$ being towards the region of higher intensity than $F_{2x}^{\text{refraction}}$, creates an imbalance in momentum transfer. The net force on dielectric particle due to imbalance in momentum transfer drags the particle towards region of higher intensity of Gaussian beam. The resultant force is

termed as gradient force. Also, the particle propagates along the beam direction due to strong on-axis scattering force.

6.3 Concept of Trap Stiffness and Corner frequency

The strength of the optical tweezers is the most important parameter. It linearly increases with the power of the trapping laser and depends on the physical properties of the trapped particle (refractive index, size and shape). The standard method to determine the trap strength is to measure the power spectrum of the thermal fluctuations in the position of the trapped particle [136]. The power spectrum of the fluctuations has a Lorentzian distribution and is given by Eq. (6.6),

$$S_x(f) = \frac{(K_B T)}{(\pi^2 \gamma)(f_c^2 + f^2)} \tag{6.6}$$

where, f_c is the corner frequency which gives a reliable measure of the trap strength [126], K_B is the Boltzmann constant, T is surrounding medium temperature, γ is Stoke's viscous drag coefficient. To enable measurement of force, the trap stiffness 'k' of an optical trap needs to be calibrated. Usually calibration is done by collecting position data as a function of time in one dimension (longitudinal or transverse) at sampling rates of few kHz and then converted into frequency information by Fourier transformation [136]. The Power Spectrum Density (PSD) is then calculated from the frequency spectrum. By measuring the corner frequencies (using PSD) in the x and y directions the trap stiffness is computed. The linear relation between the displacement "Δx" of this particle with respect to the trap center has to be determined as;

$$k = \frac{-F}{\Delta x} \tag{6.7}$$

The trap stiffness is defined as force per unit displacement. It depends on i) wavelength and power of laser, ii) refractive index of the particle and medium surrounding the particle, iii) size and shape of the particle and iv) numerical aperture and magnification of the objective lens (how tight the laser beam is focused). In power spectral analysis, the power spectrum is fit with a Lorentzian, giving rise to the corner frequency fc, which is proportional to the trap stiffness k_{trap},

$$k_{trap} = 2\pi\gamma f_c \tag{6.8}$$

where, $\gamma=3\eta\pi d$, η= 1000μNs/m^2 is the viscosity of the water at room temperature, d is the typical diameter of the particle. So the trap stiffness can be written as

$$k_{trap} = 6\pi^2 \eta d f_c \tag{6.9}$$

Usually the bandwidth of arrayed imaging sensors (camera) is much smaller than that of photodiodes, and it becomes difficult for trap calibration using power spectral analysis. In the present work, development of an off the shelf optical trapping device [127] integrated with a lateral shearing DHIM for comparison and discrimination of micro-objects has been done. The other novel feature of the developed device is the data acquisition part. Conventional data acquisition for the PSD method requires a Quadrant photodiode (QPD) which is quite expensive and costs nearly USD 700-800. An indigenously developed QPD was used in the device, using 2x2 matrix arrangement of 4 photodiodes. The developed trapping device yields trap stiffness values which are in agreement with the simulations.

6.4 Simulation of optically immobilized particle using OTGO toolbox

Before the construction of the optical tweezer, the forces on the particle were simulated for determination of laser power requirements for establishing stable traps. The optical forces on the micro-particles were computed considering geometrical optics approximation. OTGO [137, 138] (optical tweezers in geometrical optics) computational toolbox was used for this. It was found that this approximation gives reliable results in agreement to the experiments, which were conducted on polystyrene beads of 6 and 10 micrometer diameter. This toolbox contains limited geometries and shapes which can be studied under the effect of optical forces viz. one can only study spherical, ellipsoidal and cylindrical particles. In order to study more complex biological particles like red blood cells this toolbox need to be modified, which is reserved for future work. The simulated trap stiffness for the polystyrene microspheres of size 6μm and 10μm diameter is given in Table 6.1.

Table 6.1: Trap stiffness obtained by simulations using OTGO

Particle size (μm)	Trap stiffness (pN/μm) (Simulation using OTGO)	
	k_x	k_y
6	4.739	4.725
10	2.843	2.834

6.5 Development of Optical Tweezer using DVD drive pickup unit

In this work, Optical tweezer was developed by employing optical pickup unit (OPU) from a DVD burner [127]. A DVD-RW drive consist two laser diodes for their operation, one is infrared laser diode of wavelength ~780nm for reading the disks and other is red laser diode of wavelength ~650nm for writing the disks. Fig. 4.13b shows the extracted DVD pickup unit. The lens of OPU has a focal length of ~4mm with ~0.6 numerical aperture and can focus the beam down to ~1μm spot. The OPU has a lens steering mechanism consisting of two tracking coils for moving and focusing the laser beam on different tracks of compact disks. The two tracking coils controls the position of the lens in *x*-axis and *z*-axis upon passing current through them. This mechanism of beam steering and focusing was extremely useful for manipulation of the microscopic object of interest. For this purpose, a circuitry was designed to focus and steer the objective lens by supplying current (-20 mA to +20 mA) to the tracking coils in a controlled manner, the lens mounted on the tracking coil can be moved with the precision of a fraction of a micrometer. From the mean position the objective lens can be steered to 200 μm in both $-x$ and $+x$ directions. These optical pickup units (OPUs) are in fact miniature high precision optical laboratories, consisting of a laser diode, collimating and beam shaping lens, diffraction gratings, a segmented quadrant photo-detector (QPD), half wave plate and a singlet aspherical objective lens of diffraction limited quality.

Figure 6.3 shows the experimental setup for the Lateral shearing digital holography microscopy (LSDHM) of immobilized micron sized objects, corner frequency and trap stiffness measurement. The OPU was slightly modified to meet the intended purpose. The diffraction grating in OPU was removed from the optical path, increasing the output power of the central beam to ~40 mW [127]. The Red laser diode in OPU was powered by indigenously developed laser driver circuit. The infrared laser diode inside the OPU was extracted and a blue led (Luxeon star, λ=470 nm. $\Delta\lambda$=30nm) was used in its place so that it could be used for bright field microscopic imaging of trapped object. Light from the red laser diode (650nm, 250 mW) of the OPU was used for the trapping of the micron-objects. It was passed through the object (in the initial studies, polystyrene microspheres were used) and then magnified using the imaging lens. For quantitative phase imaging a green diode laser was used.

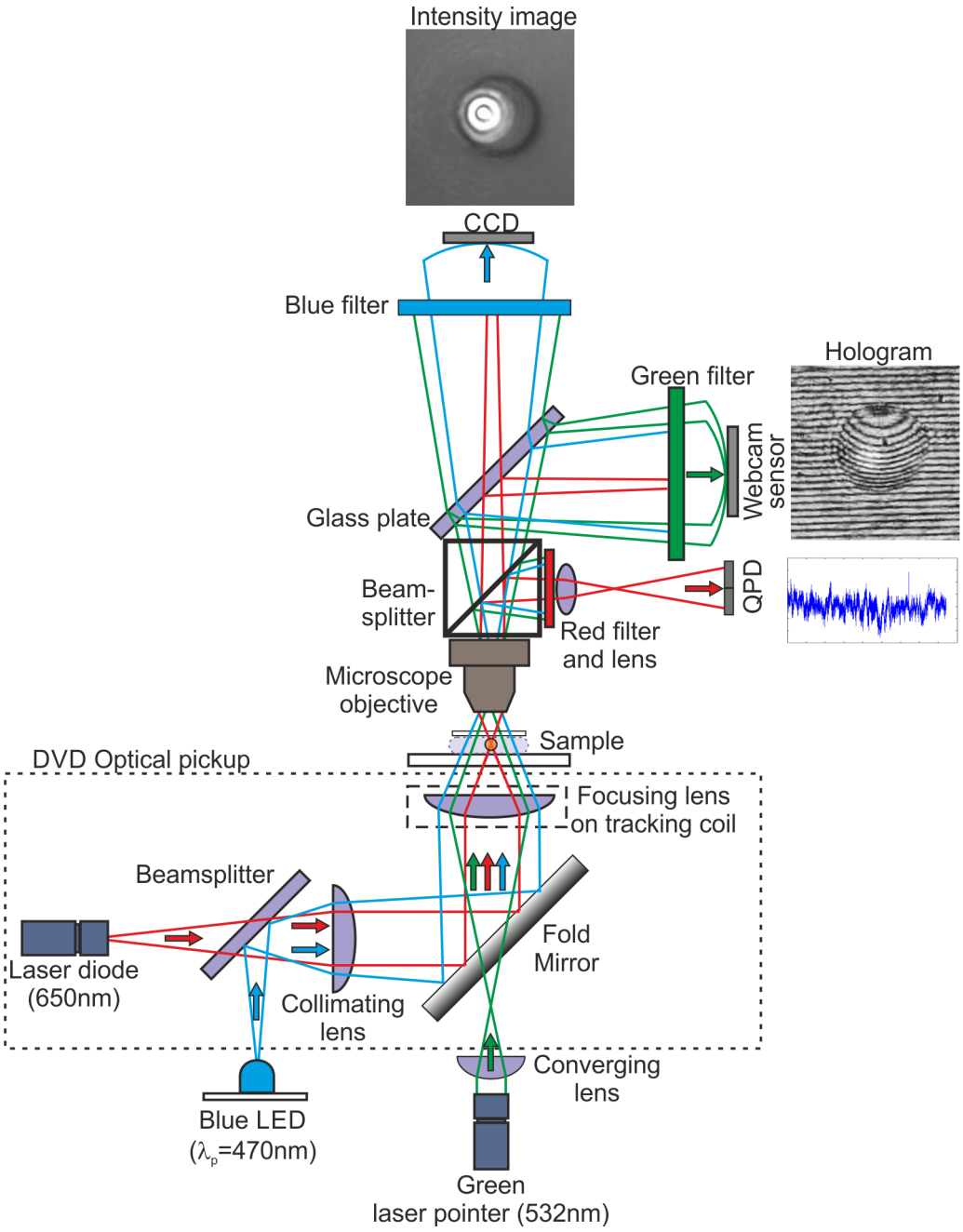

Fig. 6.3: Low cost optical tweezer integrated with lateral-shearing DHIM

Fig. 6.4 shows the photograph of the whole setup. Inside OPU, the red laser beam passes through the collimating lens and then reflected from the folding mirror, which is inclines 45° to the incident beam, the beam is then focused by the lens and forms a near-diffraction limited spot at the focus. A green laser diode (λ=532nm, 5 mW, ThorLabs.) is coupled with focusing lens of focal length 9mm and placed under the folding mirror (which is used to deflect the red laser beam from the

diode onto the objective lens of OPU), in order to produce a diverging beam which fully covers the objective lens of the OPU and forms a focal spot at a different plane in the sample.

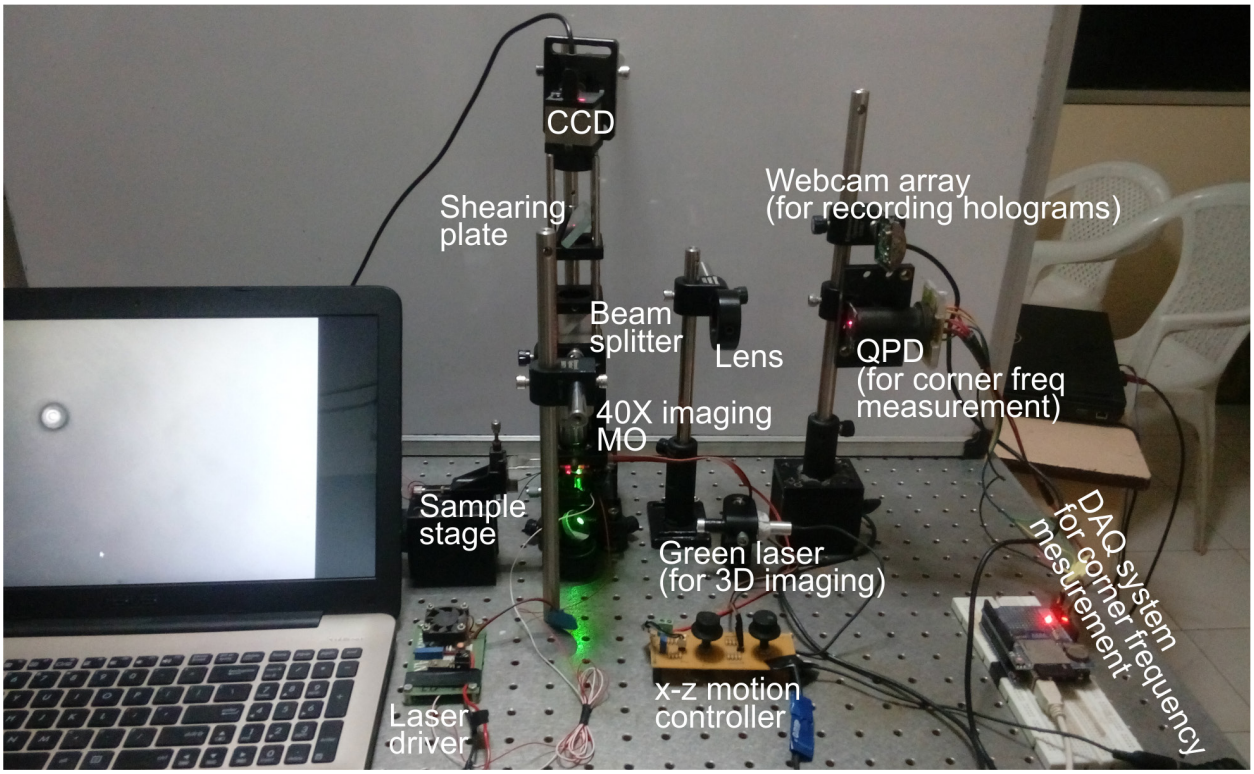

Fig. 6.4: Photograph of the Low cost optical tweezer and the necessary electronics.

The object was magnified by microscope objective lens of numerical aperture 0.65 and 45× magnification. A beam splitter having 50:50 splitting ratio was placed in the propagation direction to divide the wavefronts from all the sources into two parts, one portion of the wavefronts is directed towards the indigenously developed QPD for corner frequency measurement. A red filter was placed before the QPD to filter out the blue bright field imaging beam and the green DHIM beam and allow only the red laser beam through. A lens was used after the red filter to expand the red laser beam so as to illuminate the four quadrants of the QPD.

A green laser diode (λ=532nm, output power=5mW, ThorLabs.) was coupled with focusing lens of focal length 9mm and placed under the folding mirror (which is used to deflect the red laser beam from the diode onto the objective lens of OPU), in order to produce a diverging beam which fully covers the objective lens of the OPU and forms a focal spot at a different plane inside the sample. The transmitted green laser light carries the complete object information and was used for LS-DHIM. Two laterally sheared versions of this object wavefront after the beamsplitter were

created by a fused silica glass plate of 5mm thickness mounted at 45◦ with the incoming green laser beam. The two laterally sheared beams containing the object information, superpose at the detector plane generating the holograms (interference patterns). For sparsely prepared sample, the portion of one object wavefront (either from front or back surface of glass plate) which does not contain object information, acts as a reference for the object wavefront (either from back or front surface of the glass plate). A green bandpass filter was placed before the webcam array (24-bit, 3.2µm pixel pitch) used for recording the holograms, in order to block the red trapping beam and blue imaging beam. Detailed explanation on LS-DHIM can be found in Chapter 4.

The beam after passing through the glass plate was filtered using a blue bandpass filter, which blocked and the red trapping beam and green DHIM beam in order to prevent over exposing of sensor. A CCD array (8-bit, 4.65mm pixel pitch) was kept behind the filter for capturing intensity images of the trapped particles.

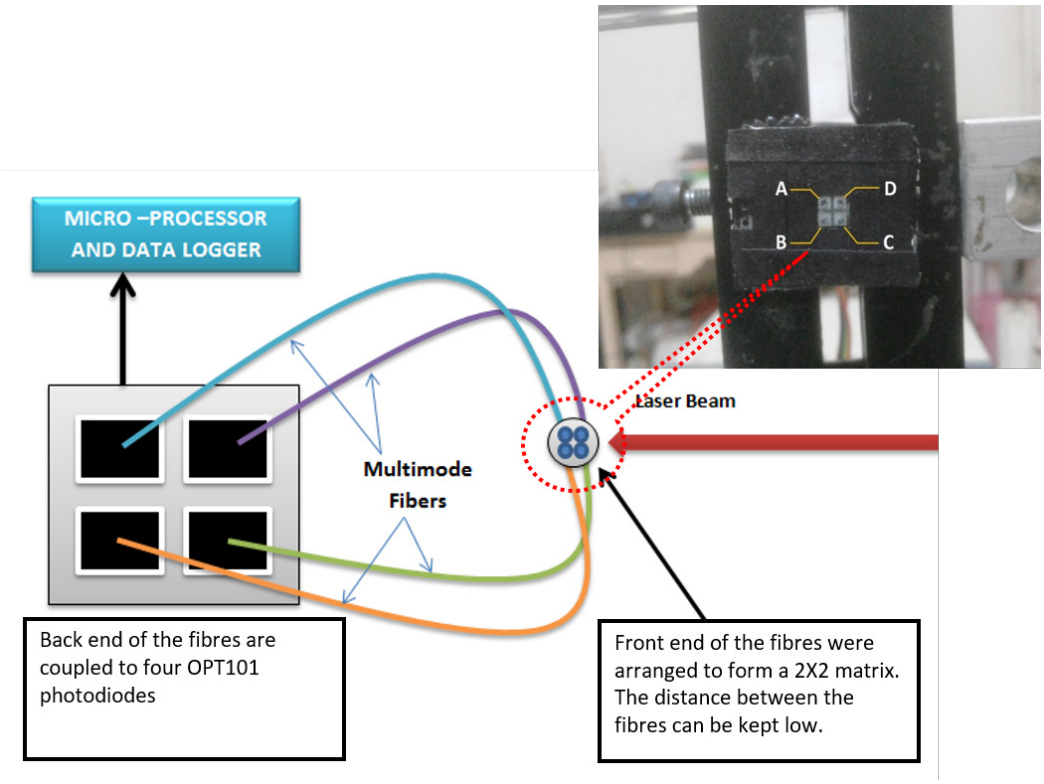

Fig. 6.5: Indigenously developed QPD for corner frequency and trap stiffness measurement

As depicted in Fig. 6.5, the quadrant photo diode was designed from four OPT101 photodiodes by a 2×2 matrix arrangement. Unlike the commercially available QPDs, the separation between the neighboring photodiodes in the designed QPD arrangement was nearly 1.5 cm due to bezels around

each photodiode. To achieve least distance between photo-diodes, the photodiodes were coupled to multimode fibers. In Fig. 6.5, A, B, C and D are the front end of the fiber cables (see Inset of the figure). The laser beam is further focused using a lens of focal length 25mm and then the photodiode matrix was kept at the best possible position, where the beam spot covers the front end of all the four fibers cables. After immobilizing the object, the output voltages from the quadrant photodiode was logged using Arduino UNO R3 development board and a SD card data logging shield. An Arduino program was written in C++ in order to achieve high sampling rate (above 10 kHz). The recorded data is further processed in computer for corner frequency (f_c) and trap stiffness (k) measurements. The laser input power was kept constant for all measurements.

6.6 Sample preparation

In this work, Polystyrene beads (polysciences inc., refractive index ~1.59) of size 10 μm and 6 μm were used initially to test the effectiveness of the developed optical tweezer. The sample was prepared by mixing polystyrene micro-spheres of required quantity with Deionized (DI) water and sodium lauryl sulphate (0.05g/ml) was added to prevent agglomeration of the beads.

For biological samples blood cells (especially red blood cells) were prepared by mixing required density of RBCs with 0.5ml phosphate buffer saline solution (PBS) and 0.5ml deionized water and centrifuged for 10 minutes. This accumulates the RBC pellets at the bottom of the test tube, the top layer containing plasma and WBCs was discarded. This process was repeated three times in PBS to remove most of the plasma and white blood cells, 0.167% of the bovine serum albumin was added to the suspension in order to prevent the adhesion of the RBCs to the walls of the sample chamber. PBS is a water based salt solution containing sodium hydrogen phosphate, sodium chloride. In some formulation, it also contains potassium chloride and potassium dihydrogen phosphate. It is commonly used for biological research. The osmolarity and ion concentration of the PBS matches with those of the human body (isotonic). PBS is non-toxic to most cells including RBCs, and helps RBCs to maintain their shape.

6.7 Trapping of polystyrene micro-spheres and red blood cells

The developed optical tweezer was used to immobilize polystyrene micro-spheres as well as red blood cells. Trapping efficiency will depends upon the incident power of the laser beam. In all the experiments the same power (~250mW) of the laser beam was used. Sequence of images shown

in Fig. 6.6 shows the movements of a 6μm diameter polystyrene bead getting immobilized by the tweezer. It was recorded by the CCD array at the rate of 20Hz. The micro-sphere can be moved around by laterally shifting the trapping beam as shown in the figure. When the trap is moved faster, the microsphere escapes from it as expected, but falls back to it, if it is not far (last to images in Fig. 6.6). In Fig. 6.6, the movement of the trap and the microsphere are represented by red and black arrows respectively. The image clearly shows that the optical tweezer made up of the DVD OPU can immobilize micro-particles.

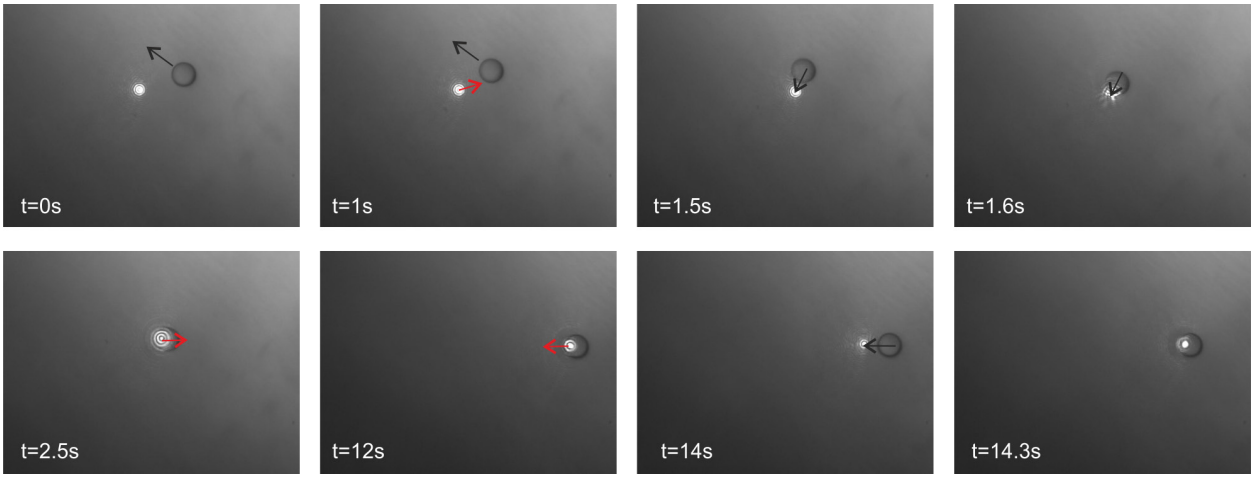

Fig. 6.6: Intensity images of immobilization of 6μm diameter polystyrene microsphere.

Flat objects like RBCs would align itself along the direction of beam propagation [OT5] in order to have maximum gradient force as shown in Fig. 6.7 (first row). Once the trap beam is switched off RBCs will flip back so that the flat surface is perpendicular to beam propagation direction.

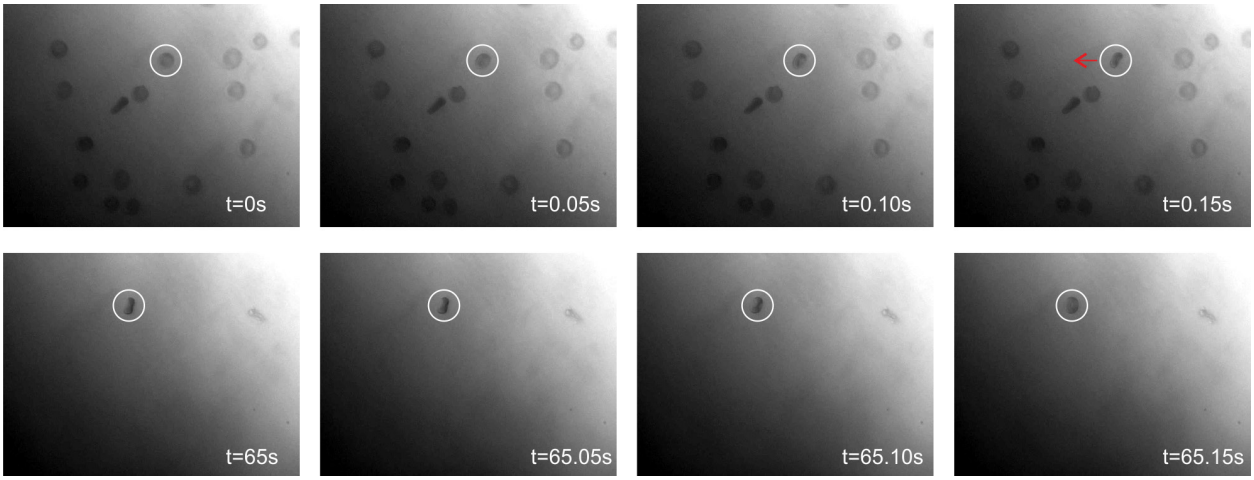

Fig. 6.7: Intensity images of optical trapping of RBCs. They flip along the direction of beam propagation.

6.8 Corner frequency and trap stiffness measurement for polystyrene beads

Objects (polystyrene beads and RBCs) when immobilized using optical tweezer, exhibits Brownian fluctuations. In optical tweezers, as described in the previous sections, the trap stiffness is directly proportional to the power of trapping beam and it also affects the mean displacement of the trapped object and frequency of fluctuations. For constant power of trapping beam, the corner frequency measurement can prove to be good discriminating parameter between objects of different shapes, size and contents. Initial experiments were conducted using polystyrene beads of 6µm and 10µm diameter. Figure 6.8 shows the raw voltage values recorded as a function of time for a 6µm sized polystyrene bead. The data shows the Brownian nature of particle movement inside the trap. The sampling rate was 10kHz and the total sampling time was around 16 second.

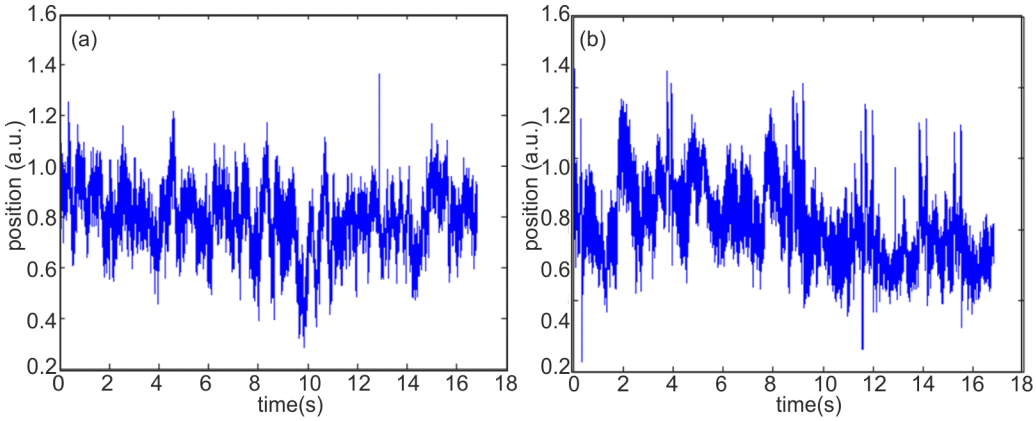

Fig. 6.8: Brownian fluctuations of the 6µm diameter polystyrene bead measured using the in-house developed QPD in (a) *x*-direction and (b) *y*-direction

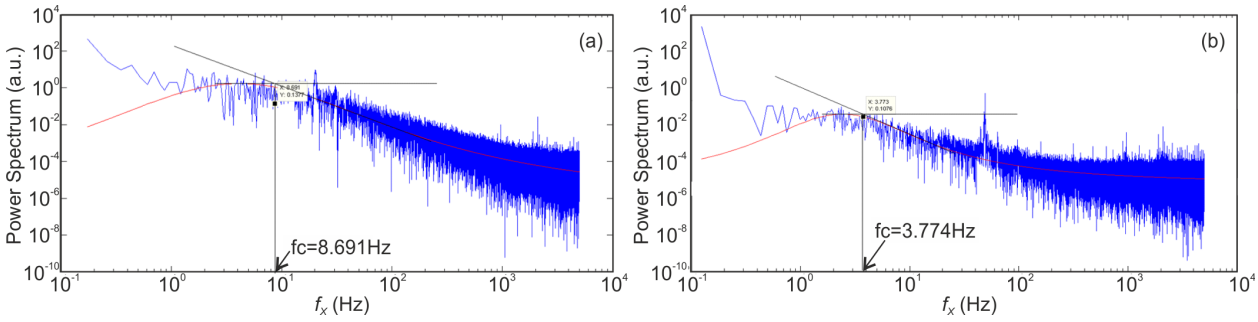

Fig. 6.9: Power spectrum for (a) 6µm diameter sphere and (b) 10µm diameter microsphere. Red line in the figures represent the Lorentzian fit.

Figured 6.8a and 6.8b shows the power spectrum (f_x) (blue curve) of the fluctuations in the case of a 6µm and a 10µm diameter polystyrene beads respectively. Power spectrum is computed from the Fourier transform of the displacement data (Brownian fluctuations). Corner frequency of the

spectrum is determined after fitting the obtained distribution by a Lorentzian function (red line in Fig. 6.8). The frequency value at the point of intersection between the tangents of the two sections of the fitted curve provides the corner frequency of the fluctuation. From Figure 6.8, it can be seen that there is a noticeable change in the corner frequencies for 6µm and 10µm diameter polystyrene beads. This is expected since for a constant laser output, the corner frequency depends on the size of the particle (Eq. 6.9). The developed technique was able to distinguish corner frequencies produced by objects of different sizes. Corner frequencies (f_{cX} and f_{cY}) were determined for 40 micro-spheres of diameter 6µm and 10µm. Figure 6.10 shows the histogram of the corner frequencies.

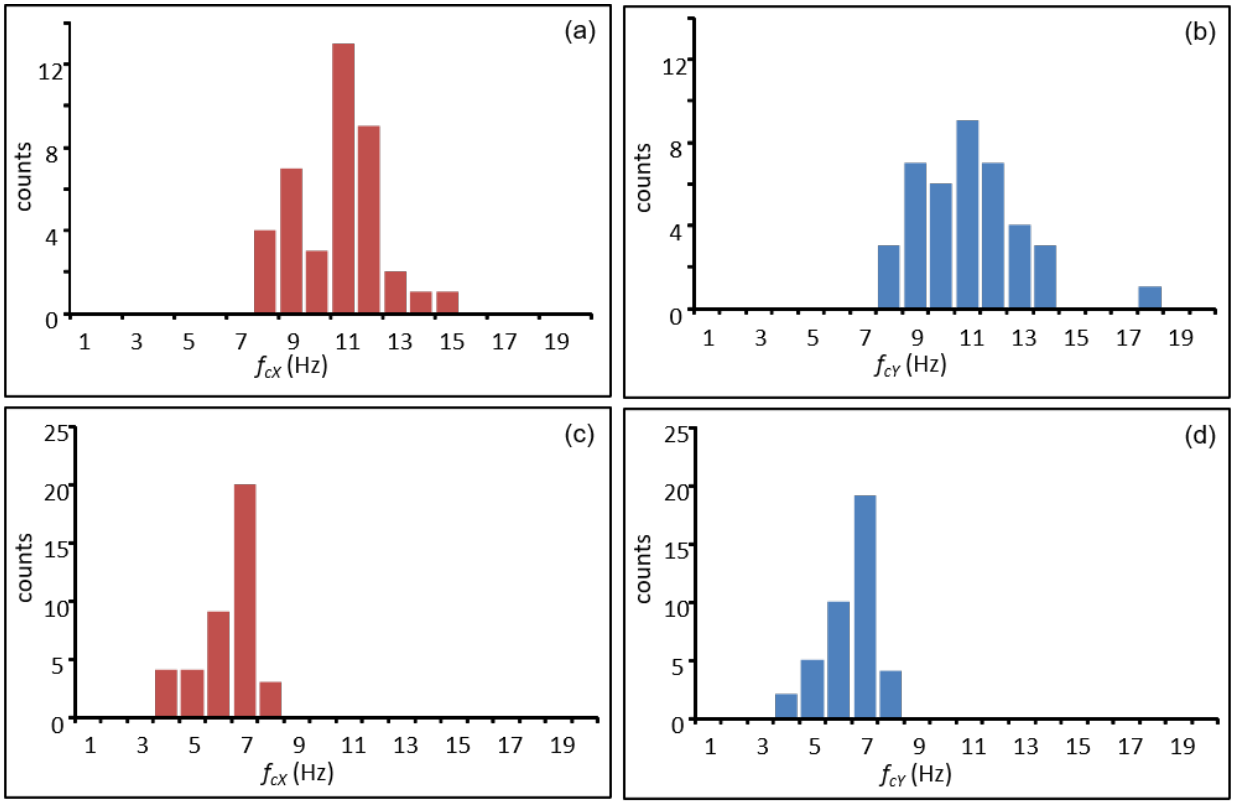

Fig. 6.10: Histogram of the corner frequencies in the (a) x-direction and (b) y-direction for 6µm diameter micro-spheres, (c) x-direction and (d) y-direction for 10µm diameter micro-spheres.

Corner frequency measurement is summarized in Table 6.2. Average and standard deviation of measured corner frequencies are given. It can be seen that the measured corner frequencies for microspheres of different diameters are different. So the corner frequency of Brownian motion of the trapped particle could act as discrimination parameter for object identification and classification. Distributions of corner frequencies for the two sets of microspheres are shown in Fig. 6.11.

Table 6.2: Measured corner frequencies using the in-house built low-cost QPD

Frequency	Corner frequency (f_c) for 6µm poly-beads		Corner frequency (f_c) for 10µm poly-beads	
	Mean (Hz)	Standard deviation (Hz)	Mean (Hz)	Standard deviation (Hz)
f_x	9.33	1.68	4.83	1.09
f_y	9.55	1.99	4.92	0.99

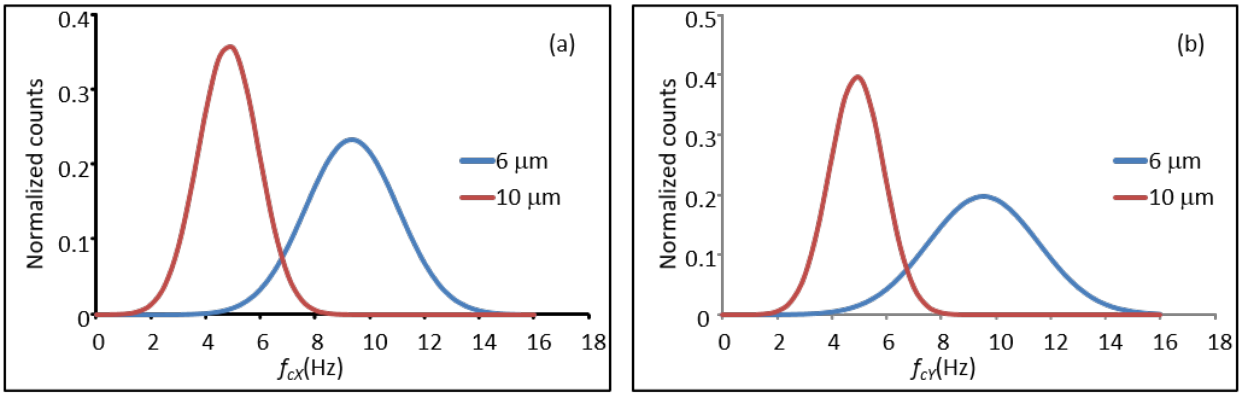

Fig. 6.11: Histogram of corner frequency distribution fitted using normal probability density function. (a) displacement in x-direction and (b) displacement in y-direction

Figure 6.12, illustrates the discrimination ability of the technique. It shows the measured corner frequency of individual objects.

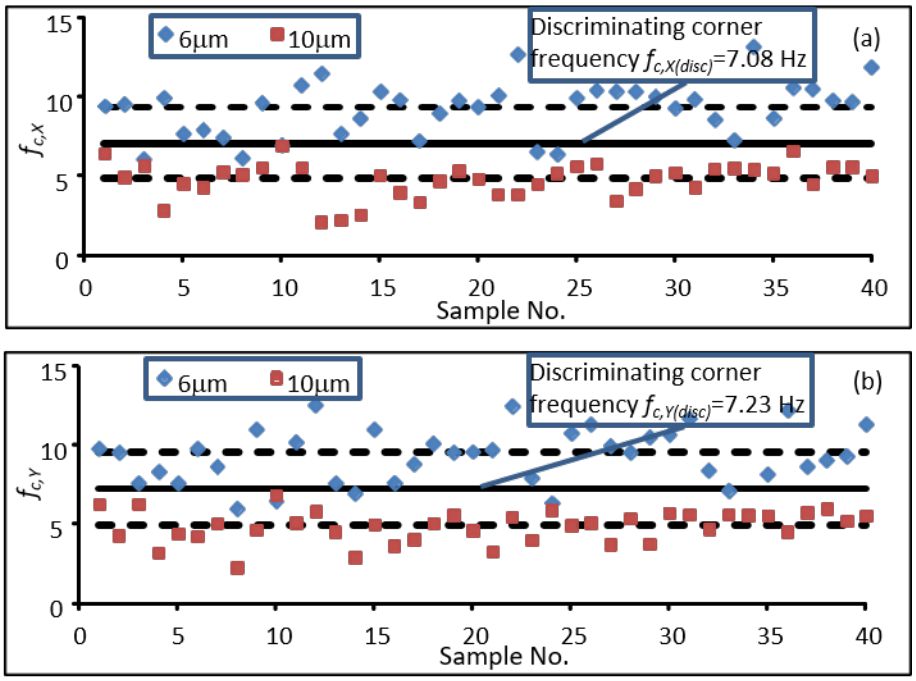

Fig. 6.12: Measured corner frequency of individual objects (a) $f_{c,X}$ and (b) $f_{c,Y}$

In Fig. 6.12a and 6.12b the continuous line is the discriminating corner frequency. It is the average of the corner frequency for 6µm and 10µm diameter micro-spheres. Mean of the corner frequencies for individual size objects are shown by dashed lines. The identification probability is given in Table 6.3

Table 6.3: Object classification using corner frequency

Rate	Identification using $f_{c,X}$		Identification using $f_{c,Y}$	
	Particle size		Particle size	
	6µm	10µm	6µm	10µm
True Positive (%)	87.5	100.0	90.0	100.0
False Positive (%)	0.0	12.5	0.0	10.0
True Negative (%)	100.0	87.5	100.0	90.0
False Negative (%)	12.5	0.0	10.0	0.0

For 6µm microsphere, TPR is computed from the number of 6µm particles correctly identified as 6µm particles, FPR is computed from number of 10µm particles incorrectly identified as 6µm particles, TNR is computed from 10µm particles correctly identified as 10µm particles and FNR from number of 6µm particles incorrectly identified as 10µm particles. Similar is the case for of 10µm spheres.

Trap stiffness was computed using the value of corner frequency in Eq. (6.9). Table 6.4 shows the trap stiffness values from experiment and simulations. It can be seen that the experimental and simulation values are very close to each other.

Table 6.4: Measured trap stiffness

Particle size (µm)	Simulation [OTGO] (µN/m)		Experiment (µN/m)	
	k_x	k_y	k_x	k_y
6	4.739	4.725	4.965	5.078
10	2.843	2.834	2.856	2.908

6.9 Integration of LS-DHIM to low-cost optical tweezer

As mentioned in the introduction of this chapter, the addition of quantitative phase imaging unit to the low-cost optical trap, will provide the user with a multitude of object parameters in addition

to its corner frequency information. Lateral shearing DHIM could be easily integrated into the trapping device, by adding a glass plate and an imaging device on to the setup (see Figures 6.3 and 6.4). As discussed in Chapter 4, for sparse object distribution and for shearing much larger than the size of the object (thick glass plates) holograms result. These holograms were recorded by a VGA webcam. Fig. 6.13 shows a series of holograms (recorded at the rate of 25Hz) of a 6μm diameter polystyrene micro-spheres suspended in DI water while it is being immobilized by the optical tweezer.

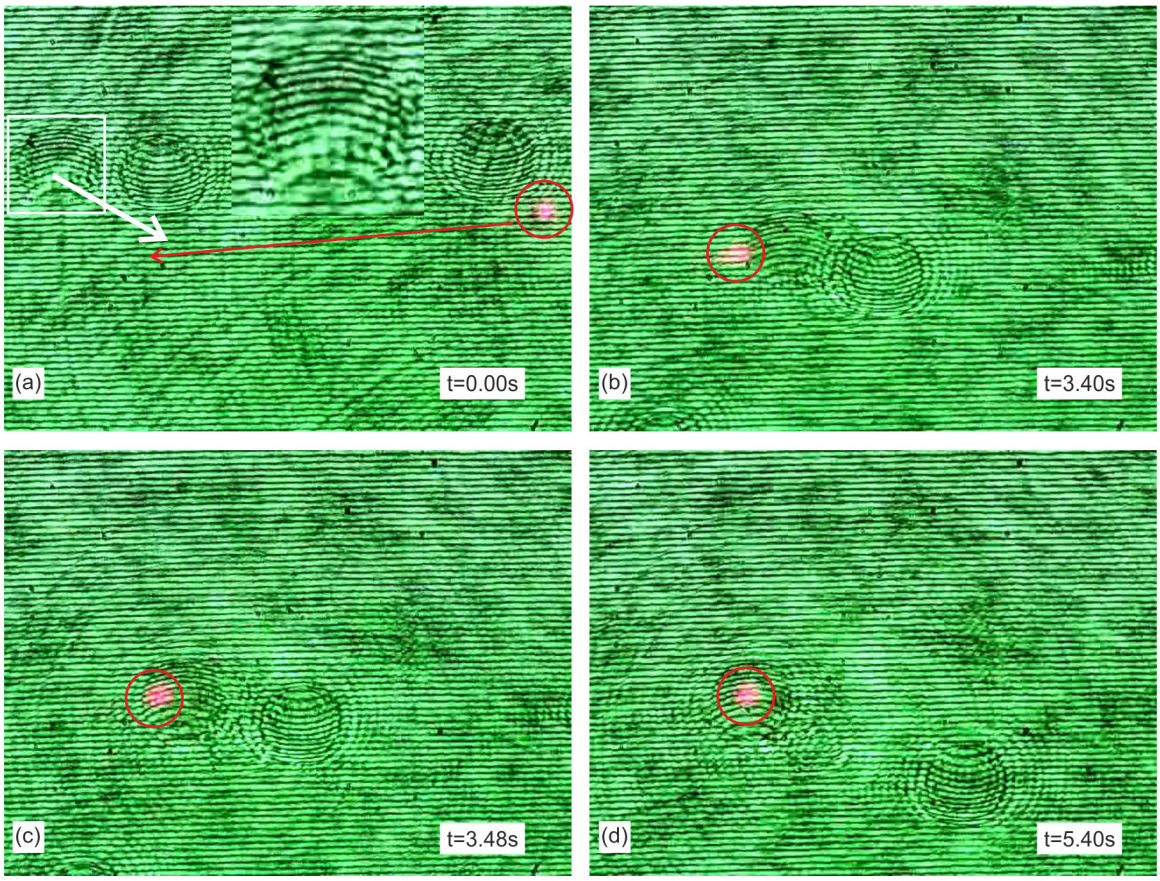

Fig. 6.13: Holograms of immobilized 6μm diameter polystyrene micro-spheres at different time instances. The trap beam is marked inside the red circle in each figure.

Each hologram is separately reconstructed using the numerical processing algorithm described in Chapter 3 and the phase profile is extracted. Phase profile is also obtained from a hologram recorded without the micro-spheres in the fields of view. This phase is subtracted from the phase profile obtained from the hologram with the micro-spheres to bring out the object phase profile, which is shown in Fig. 6.14. The phase profile shows a movement of the micro-spheres (since it

is in flowing DI water) as well as shows that the trapped micro-sphere is attracted to the high intensity region of the trapping beam.

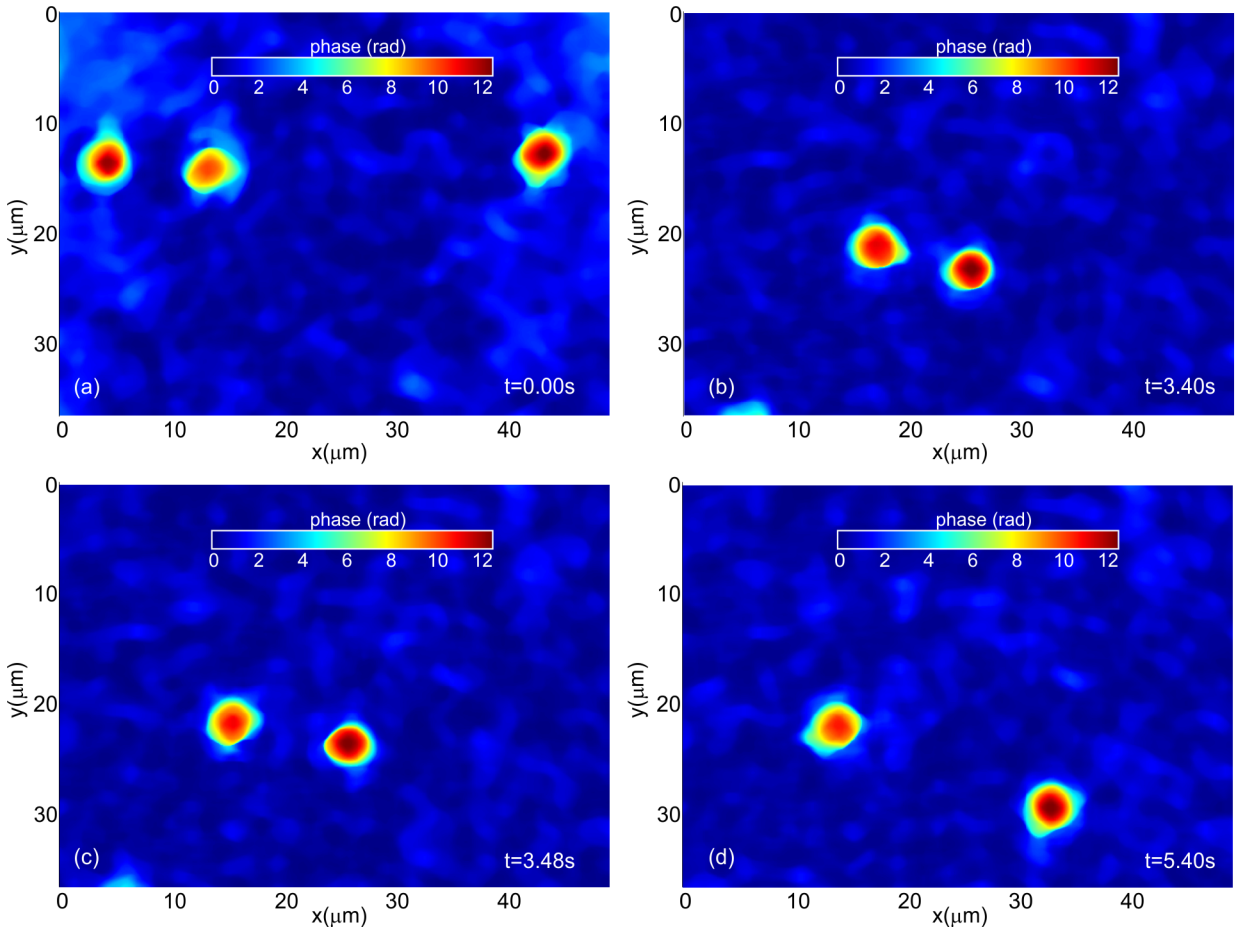

Fig. 6.14: Reconstructed phase profiles for the holograms shown in Fig. 6.13

Path length variation of the probe beam passing through the trapped micro-sphere is shown in Fig. 6.15a to 6.15e for different time instances. This computed by subtraction of the reference phase from the object phase. The changes in path length is quite evident from the figure. Brownian motion of the particle in the trap leads to large path length changes especially near the periphery of the object. The standard deviation of the path length variation with time (for 15s) at each point on the object was computed and this acted as the measure of the path length fluctuation at each space point. This is shown in Fig. 6.15f. From this figure it can be seen that the path length fluctuation near the edge of the microspheres is more. Also the mean of the computed optical path length flotation was about 50nm, which is on the higher side, because of the Brownian motion of the suspended particle. In the case of biological samples this fluctuation will be the sum of surface thickness change and fluctuation due to Brownian motion.

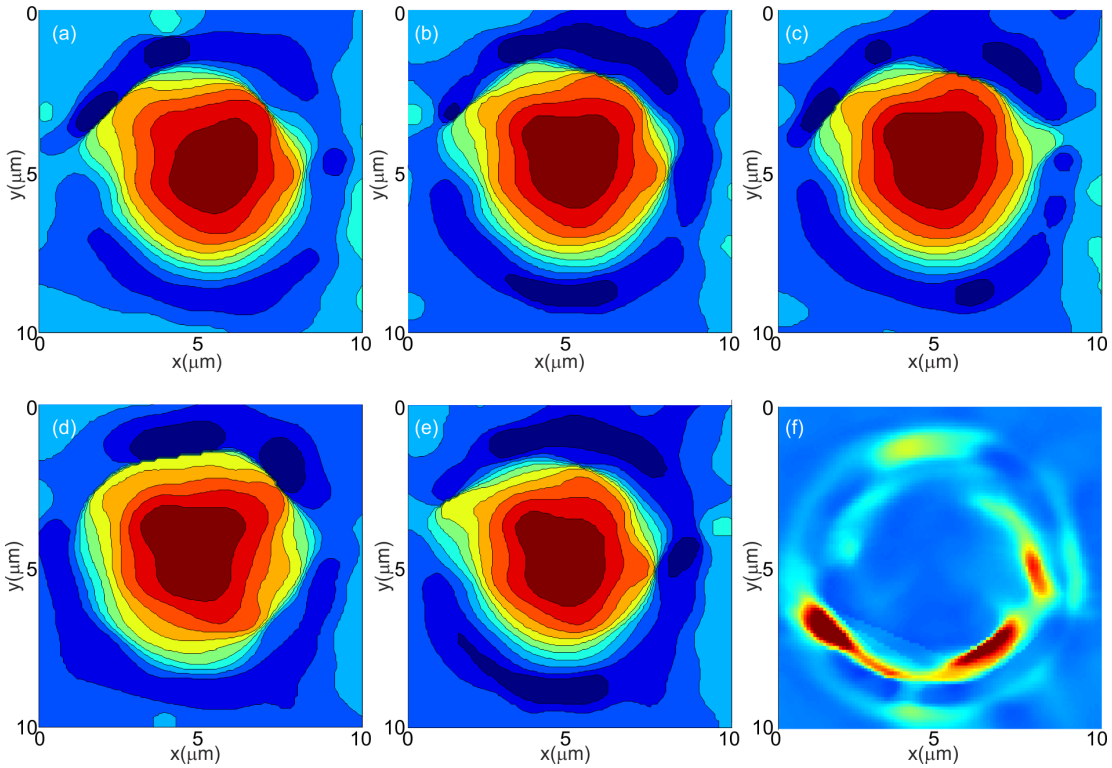

Fig. 6.15: Contour plots of thickness profile of the object at different time instances (a) 0s, (b) 3s, (c) 6s, (d) 9s and (d) 12s. The thickness fluctuation profile computed from time varying thickness for the entire acquisition time (15s) is shown in (e).

The experiments were carried out on RBCs suspended in PBS. Fig. 6.16a shows the hologram of trapped RBC (which has flipped along its axis). Fig. 6.16b shows the phase profile of the trapped RBC computed after phase subtraction.

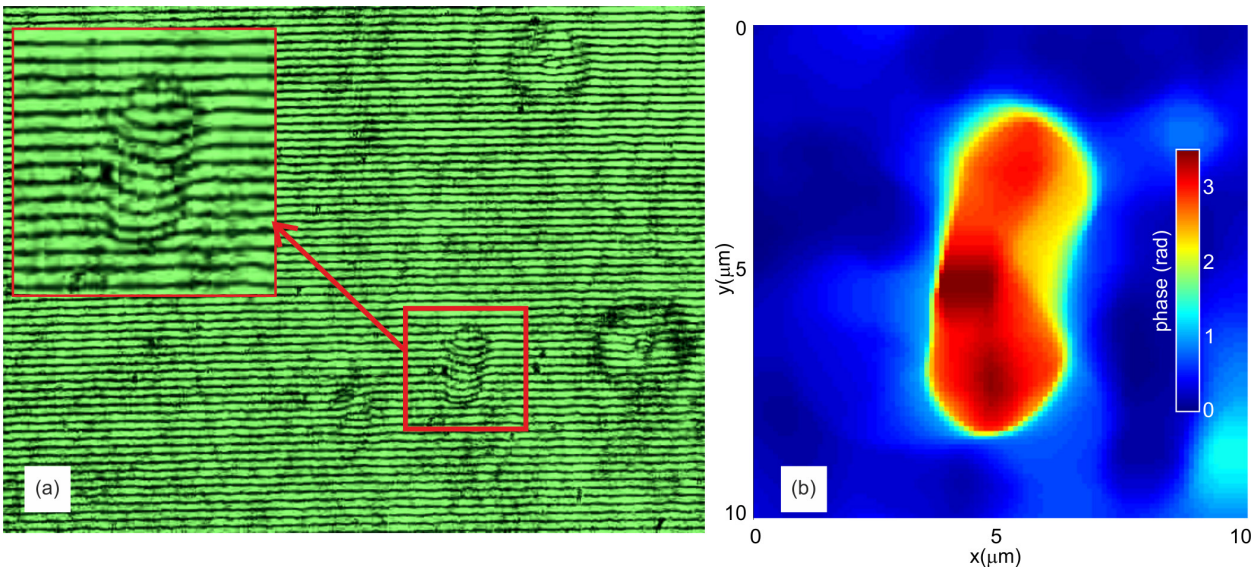

Fig. 6.16: (a) Hologram of a RBC trapped by the optical tweezer. Inset of the figure shows detailed view of the modulated interference fringes due to the trapped RBC. (b) Reconstructed phase profile of the trapped RBC obtained after phase subtraction.

In the case of RBCs the measure optical thickness fluctuations were above 60nm, which basically is due to both the thickness fluctuation and the Brownian motion. Also rotations of the RBC were also observed, which is due to polarization state of the trapping beam [139].

6.10 Conclusions

A low cost optical trap along with an indigenously developed QPD were used to measure corner frequencies of trapped micro-objects. A lateral shearing DHIM was integrated on to the system to measure morphology changes of trapped objects. The in-house developed low cost QPD and data acquisition system was found to measure the corner frequencies and trap stiffness accurately. Corner frequency itself contains important information on the size, shape and content (refractive index) of the trapped object. In addition to the corner frequency the developed system could measure object morphology also. This leads to measurement of morphological (both physical and mechanical) parameters of objects trapped by the optical tweezer. This combination can be used to study cell morphology and its time variation of immobilized particles in fluids. Also the addition morphological information along with corner frequency and its time evolution can shed more information on the shape and content of the cell (which may depend upon its state of health), which then can be used for cell identification, discrimination and sorting.